Northern Hemisphere stratospheric winds in higher midlatitudes: longitudinal distribution and long-term trends

Michal Kozubek, Peter Krizan, Jan Lastovicka

Institute of Atmospheric Physics ASCR, Bocni II, 14131 Prague, Czech Republic
Correspondence to: M. Kozubek (kom@ufa.cas.cz)

Abstract

The Brewer-Dobson circulation (BDC, mainly meridional circulation) is very important for the stratospheric ozone and, thus, for the overall state of the stratosphere. There are some indications that the meridional circulation in the stratosphere could be longitudinally dependent, which would have an impact on ozone distribution. Therefore, we analyze here the meridional component of the stratospheric wind at northern middle latitudes to search for its longitudinal dependence. The analysis is based on the NCEP/NCAR-1 (National Centers for Environmental Prediction and the National Center for Atmospheric Research), MERRA (Modern Era-Retrospective Re-Analysis) and ERA-Interim (European Centre for Medium-Range Weather Forecasts (ECMWF) Re-Analysis Interim) reanalysis data. The well-developed, two-core structure of strong but opposite meridional winds, one at each hemisphere at 10 hPa at higher northern middle latitudes, and a less-pronounced five-core structure at 100 hPa, are identified. In the peak areas of the two-core structure the meridional and zonal wind magnitudes are quite comparable. The two-core structure at 10 hPa is practically identical for all three different reanalyzes in spite of the different time periods covered. The two-core structure is not associated with tides. However, the two-core structure at the 10 hPa level is related to the well-pronounced Aleutian pressure high at 10 hPa. Zonal wind, temperature and the ozone mixing ratio at 10 hPa also exhibit the effect of the Aleutian high, which thus affects all parameters of the northern middle stratosphere. Long-term trends

in the meridional wind in the "core" areas are significant on the 99% level. Trends are negative during the period of ozone depletion development (1970-1995), while they are positive after the ozone trend turnaround (1996-2012). They are independent of the Sudden Stratospheric Warming (SSW) occurrence and the Quasi-Biennial Oscillation (QBO) phase. The influence of the 11-year solar cycle on stratospheric winds has been identified only during the west phase of QBO. The well-developed two-core structure in the meridional wind illustrates the limitations of application of the zonal mean concept in studying stratospheric circulation.

1. Introduction

Stratospheric winds play an important role in stratospheric chemistry through the transportation of long-lived species, but they could also create transport barriers - which could isolate the polar vortex in winter (Shepherd, 2007, 2008). Simultaneously with the chemical processes, the trace gas distribution modulates the radiative forcing in the stratosphere. The changes of stratospheric wind, namely the strengthening of the westerly polar vortex and its poleward shift, are coupled with ozone depletion and temperature changes (Scaife et al., 2012). For example, the unprecedented ozone loss in the Arctic in 2011 was caused by extreme meteorological conditions (e.g., Pommereau et al., 2013). The Antarctic ozone hole intensification over the 1980–2001 period is not solely related to the trend in chemical losses, but more specifically to the balance between the trends in chemical losses and ozone transport (Monier and Weare, 2011a). One of the most studied circulation structures in the stratosphere is the BDC. A detailed description of this circulation can be found in Butchart (2014). Many model studies reveal an acceleration of the residual mean circulation and the BDC due to increasing greenhouse gas (GHG) concentration (Oberlander et al., 2013; Lin and Fu, 2013; Oman et al., 2009). However, the age of air data does not confirm a simple pattern of

reduction of the age of air as a consequence of the Brewer-Dobson circulation intensification (Engel et al., 2009; Stiller et al., 2012). Monier and Weare (2011b) found some weakening of the northern winter BDCin polar region in reanalysis ERA-40 (ECMWF Re-analysis for 40 years) and R-2 (NCEP-DOE Reanalysis 2). Some changes of stratospheric wind (strengthening of the westerly polar vortex and its poleward shift, changes in the BDC) are coupled with ozone depletion and also temperature changes. Possible interactions between changes in the stratospheric dynamics and climate changes in the troposphere have been described by Hartmann et al. (2000), Scaife et al. (2012) and Deckert and Dameris (2008). The stratospheric QBO and downward feedback from the stratospheric vortex to tropospheric weather systems have been reported to be relevant both in the context of weather prediction and climate (Baldwin and Dunkerton, 1999; Baldwin et al., 2003; Sigmond et al., 2008; Marshall and Scaife, 2009; Wang and Chen, 2010). Moreover, stratospheric wind (zonal and meridional) affects vertically propagating atmospheric waves, which control the transport circulation in the stratosphere and mesosphere (Holton and Alexander, 2000).

It is generally accepted that the meridional wind component in the stratosphere is much weaker than the zonal wind component. However, as we show later, it is not always the case. Many studies have been working with zonal mean winds. The Northern Hemisphere has a pronounced distribution of continents, mountain regions and oceans, which is reflected in the troposphere and also in the stratosphere. Some phenomena introduce longitudinal differences into wind pattern, for example the El-Nino Southern Oscillation - ENSO (e.g., Weare, 2010). The total ozone in the winter higher middle latitudes has a strong longitudinal dependence, the maximum-minimum difference being more than 100 D.U. (e.g., Mlch, 1994). Demirhan Bari et al. (2013) found longitudinal dependence of residual winds in the stratosphere and, through impact on the BDC, some effects on stratospheric ozone and water vapor in the stratosphere for 2001-2006 (changes in distributions and concentration).

Therefore, there are reasons for studying longitudinal dependence of meridional wind and other parameters in the stratosphere based on the long-term re-analysis data series – which is the aim of this paper.

Our study of longitudinal distribution of meridional and zonal wind, which we found to be substantial, should reveal where the meridional wind is a substantial component of the total horizontal wind. The results could have an impact on Brewer-Dobson circulation in terms of longitudinal distribution, which is very important for ozone transport in the stratosphere. The distribution of meridional wind is very important for wave propagation in the stratosphere (Matsuno, 1970, Kodera et al., 1990). Therefore, here we investigate longitudinal distribution of meridional and also zonal component of stratospheric winds at northern middle latitudes. The impact of QBO or SSWs, which is mainly wave driven, is also studied.

To test the temporal stability of longitudinal distribution, long-term trends at latitudes of the most pronounced longitudinal structures are calculated. Ozone concentration in the northern middle latitudes changed its trend in the mid-1990s (e.g., Harris et al., 2008). Since ozone is the main heater of the stratosphere via absorption of solar radiation, this turnaround of ozone trend had to also affect, more or less, the behavior of other stratospheric parameters, and it affects even the mesosphere and lower thermosphere (e.g., Lastovicka et al., 2012). Since ozone trends in the northern middle latitudes changed in the mid-1990s (e.g., Harris et al., 2008), trends in the stratospheric dynamics are expected to be altered by the ozone recovery and thus trends in the periods before and after the mid-1990s are examined separately.

SSW and QBO are known to have an important impact on the stratosphere, including its circulation (Limpasuvan et al. 2004, Naito and Hirota, 1997, Labitzke and van Loon, 1988). The stratosphere is also influenced by solar activity (e.g., Gray et al., 2010 and

104 references herein). Impact of these phenomena on stratospheric circulation, particularly on the
105 observed longitudinal structures in meridional wind, deserves attention and analysis.
106 This paper focuses on two topics:
107 (1) Longitudinal distribution of the meridional wind component at different pressure
108 levels and the possible reasons for its behavior. Therefore the longitudinal distributions of
109 geopotential height and zonal wind component will also be calculated. This will be
110 accompanied by trend analysis of observed longitudinal structures. The results are described
111 in Section 3.1. Long-term trends in the longitudinal distribution of meridional wind are also
112 examined and the results are presented in Section 3.2.
113 (2) Trend analysis of stratospheric total horizontal wind and meridional component
114 with connection to QBO, SSW (mainly wave driven) and solar activity. The results are
115 described in Section 3.3.
116 The structure of the paper is as follows. In Section 2, the data and methods are
117 described. Then, in Section 3, the results of analysis are shown and, in Section 4, they are
118 briefly discussed. Section 5 summarizes conclusions.
119
120 **2. Data and methods**
121
122 Stratospheric winds have been measured from the ground using active and passive techniques
123 (Hildebrand et al., 2012; Rüfenacht et al., 2012). From space they were measured by the High
124 Resolution Doppler Imager (HRDI) on the Upper Atmospheric Research Satellite UARS
125 covering 10–35 km and 60^{o}S–60^{o}N, using the molecular oxygen A- and B-bands (Ortland et
126 al., 1996). Baron et al. (2013) derived winds from SMILE (Superconducting Wave Limb
127 Emission Sounder). However, direct wind measurements do not provide sufficiently long and
128 homogeneous global data series.

Therefore when studying longitudinal distribution of meridional or zonal wind, we use three independent reanalysis data, namely reanalyzes NCEP/NCAR-1 (National Centers for Environmental Prediction and the National Center for Atmospheric Research, further on NCEP/NCAR), MERRA (Modern Era-Retrospective Re-Analysis) and ERA-Interim (European Centre for Medium-Range Weather Forecasts (ECMWF) Re-Analysis Interim). The NCEP/NCAR reanalysis was described in detail by Kistler et al. (2001). This reanalysis provides data from 1948 onwards (but the data is more reliable from 1957 onwards, when the first upper-air observations were established) and from 1979 onwards, due to the start of satellite data assimilation. Data is available on the 2.5° to 2.5°grid at 00, 06, 12 and 18 UTC. Vertical resolution is 28 levels with the top of the model at 2.7 hPa. The NCEP/NCAR reanalysis system efficiently assimilates upper-air observations but is only marginally influenced by surface observations because model orography differs from reality (Kistler et al., 2001). The ERA-Interim is described by Dee et al. (2011). Data is available from 1979 on the 0.75° to 0.75°grid at 00, 06, 12 and 18 UTC. Vertical resolution is 60 levels with the top of the model at 1 hPa. The MERRA reanalysis is described in and downloaded from http://disc.sci.gsfc.nasa.gov . Data is available from 1979 on the 1.25° to 1.25°grid at 00, 06, 12 and 18 UTC. Vertical resolution is 42 levels with the top of the model at 0.1 hPa.

According to Kozubek et al. (2014), stratospheric winds from the NCEP/NCAR reanalysis are better for long-term trend analysis than those from ERA-40 and ERA-Interim reanalysis - if we take into account the length of available period. Neither ERA-40, nor ERA-Interim, nor MERRA separately cover the whole period 1958-2012. On the other hand, general pattern and long-term changes of stratospheric winds in NCEP/NCAR, ERA-40 and ERA-Interim reanalyzes (except for the last four years of ERA-40) are very close to each other since about 1970 (Kozubek et al., 2014), therefore it is sufficient to use only one of these three reanalysis for trend analysis. The 10.7cm solar radio flux (from

http://www.esrl.noaa.gov/psd/data/correlation/solar.data) is used for the solar cycle analysis (solar max and solar min). The QBO data at 50 hPa is taken from http://www.geo.fu-berlin.de/en/met/ag/strat/produkte/qbo/ and SSW data is taken from http://www.geo.fu-berlin.de/en/met/ag/strat/produkte/northpole/index.html

For the investigation of longitudinal distribution of meridional wind, zonal wind or geopotential height we have computed averages throughout the period 1970-2012 for every grid point from 20°N to 60°N and for every month. Analysis of the wind speed distribution in 100 hPa (where we can identify influence of troposphere and study dynamics near tropopause) and 10 hPa (which is a representative level for the middle stratosphere and major stratospheric warming determination) at 00 UTC or the meridional wind speed distribution at 00, 06 and 12 UTC (for examining possible influence of diurnal and semidiurnal tides) has been done for all three reanalyzes.

The trend analysis is focused on middle latitudes (50°- 60°N), again at the pressure level of 10 hPa, in order to investigate the behavior of wind in the two-core structure area. We also analyze the connection between QBO, SSW and solar activity versus dynamics (stratospheric wind) 10 hPa. In trend analyzes we have used either total horizontal wind or v (meridional) components separately. The total horizontal wind speed is calculated from gridded u (zonal) and v (meridional) components.

The selected latitudes are separated into four sectors (100°E-160°E – poleward wind core, 160°E-140°W- the sector of the Aleutian height, 140°W-80°W – equatorward wind core and 80°W-100°E – the sector not affected by the two-core structure, see Fig. 1).

We look for trends or differences between different groups in each sector at 10 hPa. The statistical significance threshold of trends has been set on the 95% level, which is the standard significance level for analyzes in meteorology (wind, temperature, etc.), and in trend analysis also on the 99% level. We divide data of the whole period into several groups

179 according to QBO (east or west QBO phase) or solar cycle influence (solar maximum years
180 and solar minimum years) and for the trend analysis we divided data into two periods (1970-
181 1995, with decreasing ozone, and 1995-2012, with increasing ozone). We compute trends
182 separately for all these groups with a significance threshold of 95% or 99%.

183

184 **3. Results**

185 *3.1 Longitudinal distribution of stratospheric meridional winds*

186 The whole period averages of meridional wind component for each grid point from
187 60°N to 20°N for January at 10 hPa have been computed. For comparison we have computed
188 these averages for three reanalyzes (MERRA for period 1979-2012, ERA Interim for 1979-
189 2012 and NCEP/NCAR for 1958-2012). The results are shown in Fig. 1. The top panel shows
190 results for NCEP/NCAR, the middle panel for ERA Interim and the bottom panel for MERRA
191 reanalysis. The behavior of different reanalyzes is quite similar in major features despite the
192 different length of time intervals. Figure 1 reveals at 10 hPa for January a core of strong
193 poleward wind on the eastern hemisphere at the middle and higher latitudes. This poleward
194 wind changes into equatorward wind core on the western hemisphere at 10 hPa (at a similar
195 amplitude as on the eastern hemisphere). Both the poleward and equatorward peaks (centers
196 of the cores in Fig. 1) are statistically significant at the 99% level for NCEP/NCAR
197 reanalysis. The results of similar analysis for 100 hPa are shown in Fig. 2. Generally, winds
198 are stronger at 10 hPa (up to 20 m/s) than at 100 hPa (up to 10 m/s). At 100 hPa there is a
199 five-core structure, which is much less pronounced than the two-core structure at 10 hPa. The
200 same analysis as in Fig. 1 is shown in Fig. 3 for July at 10 hPa. Figure 3 reveals no two-core
201 structure at 10 hPa for summer - it occurs only in winter. Winds in July are weaker than in
202 January and the distribution is much less compact compared with January. We have done the

same analysis for the higher pressure level of 5 hPa (not shown here) and the differences between the eastern and western hemispheres (two-core structure) have been found to grow with increasing height.

Figure 4 shows climatology based on the NCEP/NCAR reanalysis over the period 1958-2012 for January at 10 hPa pressure level for data from 00 UTC (top panel), 06 UTC (middle panel) and 12 UTC (bottom panel). There are almost no differences in the main features. Therefore, we can conclude that the two-core structure with opposite meridional winds is not caused by diurnal or semidiurnal tides. The other possibility for this structure could be dynamical reasons, which are discussed in the next paragraph.

Wind field is closely associated with the distribution of geopotential height because of dynamical reasons. Figure 5 shows a distribution of geopotential height at 10 hPa - again for all three reanalyzes. The Aleutian pressure high centered at about 40°-55°N, 180°E is well developed at 10 hPa. This height can block the zonal winter eastward winds. This should result in poleward meridional flow on the front side and an equatorward meridional flow on the backside side as a consequence of the flow along the strong anticyclone. Such a flow coincides with the observed two-core structure at 10 hPa with the poleward meridional component of wind on the eastern hemisphere and the equatorward meridional component on the western hemisphere. The behavior of zonal wind at 10 hPa, shown in Fig. 6 for all three reanalyzes, reveals substantial weakening of zonal wind in and around the region of the Aleutian pressure height; together with strengthening of the meridional component, it results in non-zonal, oblique wind flow. In some locations like 60^{o}N, 135^{o}E both wind components are approximately equal. The summertime distribution of geopotential heights at 10 hPa does not display any well-pronounced structure and, therefore, no pronounced structure is developed in meridional wind (Fig. 3). At 100 hPa on the western hemisphere (not the eastern hemisphere) the distribution of geopotential height resembles the five-core structure in winds

228 in Fig. 2 but, again, this structure is much less pronounced than that at 10 hPa (not shown
229 here).

230 *3.2. Trends in meridional wind cores*

231 This analysis is focused on latitudes where the two-core structure at 10 hPa was
232 identified (50°N-60°N). It is based on the NCEP/NCAR reanalysis only. The trends in
233 meridional wind are shown in Table 1. We can identify change of the trends in all four sectors
234 from a positive trend (core strengthening) for period 1970-1995 to a negative trend (core
235 weakening) for 1996-2012. The trends in core sectors (100°E-160°E and 140°W-80°W) are
236 significant on the 99% level for 1995-2012, and predominantly on the 95% level for 1970-
237 2012. Trends in the other two sectors are much smaller and statistically insignificant. The
238 turnaround of trends in total columnar ozone in the northern middle latitudes in the mid-1990s
239 (e.g. Harris et al., 2008) has an evident impact on the meridional wind cores – trends in cores
240 also alter, they change from positive before the ozone trend turnaround to negative after. We
241 are not going to speculate as to what extent this turnaround of meridional wind trends is
242 caused by dynamical factor, which is the main cause of the ozone trend turnaround. However,
243 impact of some external factors on trends in wind is investigated in the next section.

244 *3.3. Impact of solar cycle, SSW and QBO on trends in wind*

245 Further analysis (NCEP/NCAR reanalysis only), which has been done, is comparison
246 between years in the solar cycle maximum and minimum in different QBO phases and trends
247 in different dynamics situations (SSW or no SSW years, east or west QBO years). This
248 analysis is also focused on latitudes where the two-core structure at 10 hPa was identified
249 (50°N-60°N). It should reveal potential connections between solar cycle, stratospheric
250 dynamics (wind speed) and wave activity driven SSW, all under the potential influence of
251 QBO. Stratospheric dynamics and chemistry is influenced by changes in ozone concentration

252 (see e.g. Table 1), so we analyze separately wind in the periods 1970-1995, with decreasing
253 ozone, and 1995-2012, with increasing ozone. Trends are shown for different groups (with
254 and without major SSW years and east or west QBO phase years) for December-February
255 (DJF), as the strongest two-core structure occurs in January. We analyze the total horizontal
256 wind as well as meridional component separately to find out which component is more
257 affected by different drivers. The trends for meridional wind are shown in Table 2. We can
258 identify a turnaround of the trends in all four sectors for all four groups (positive one for
259 period 1970-1995, negative one for 1996-2012). There is little, if any, systematic difference in
260 trends between years with and without SSWs; perhaps the significant trends are a little bit
261 stronger in the years with SSWs. Similar conclusions can be drawn for the impact of QBO;
262 there is little dependence of trends on QBO, with perhaps a bit stronger trends for the west
263 phase of QBO.

264 The trends are significant on the 99% level (in a few cases only on the 95% level) in
265 the two sectors where the core structure occurs (100°E-160°E and140°W-80°W). There are
266 only a few significant trends (95% level) in the other two sectors. There are generally stronger
267 negative significant trends (99% level) in Table 1 than in Table 2 during the second period
268 (1996-2012) in the core-containing sectors.

269 The results of the connection of solar cycle and QBO with the total horizontal wind
270 speed are shown in the top panel of Table 3. At 10 hPa we can observe a positive difference
271 (of 2-5 m/s) between solar minimum and maximum for the west QBO in both sectors where
272 cores occur. The differences are significant at the 95% level. The differences are smaller and
273 insignificant in the other two wind sectors. The east QBO does not reveal a systematic or
274 significant difference. Moreover, sometimes wind in solar maximum is stronger than in solar
275 minimum. We can observe negative differences between the QBO east and QBO west phase
276 in solar minimum (up to 3 m/s) in all studied sectors. These differences are, again, mainly

277 significant in the two core sectors. Differences between the QBO east and QBO west phase in
278 solar maximum are mainly positive but insignificant.

279 The bottom panel shows the same analysis as the top one but for the v (meridional)
280 wind component. The differences are smaller than for the total horizontal wind. We cannot
281 find any specific features for all four groups. We can see only a few significant values in
282 different sectors.

283 The analysis was also done for each month separately and the biggest differences have
284 been found in December and January. These results show that solar activity influences the
285 total horizontal wind (i.e. mainly zonal wind) mostly in higher parts of the stratosphere (10
286 hPa) and predominately in the two core sectors (not shown in the paper).

287

288 **4. Discussion**

289 The results on longitudinal distribution of the meridional and zonal components of
290 stratospheric wind show that the meridional wind forms a well pronounced two-core structure
291 at 10 hPa in winter. This two-core structure is revealed by NCEP/NCAR, ERA-Interim and
292 MERRA reanalyzes in a very similar form, despite the different time periods used (Fig. 1).
293 The wintertime longitudinal distribution at 10 hPa can be explained neither by diurnal, nor by
294 semidiurnal tides, because there are no differences between the longitudinal distribution of
295 meridional winds at 00, 06 and 12 UTC (Fig. 4). However, the geopotential height analysis
296 reveals the reason for this longitudinal distribution. The well-developed large Aleutian high at
297 10 hPa in Fig. 5 can block the zonal flow (see Fig. 6) and pushes the winter eastward winds to
298 flow with a substantial poleward component on the western side of the Aleutian pressure high
299 and back, equatorward, on its eastern side. A comparison of Figs. 1 and 6 shows that the zonal
300 component of stratospheric wind is almost equal to the meridional component in some areas

in the cores. This phenomenon could result in the wave propagation changes in this part of the stratosphere (at 10 hPa, i.e. Matsuno, 1970, Kodera et al., 1990) and could affect other wave driven phenomena like SSW. The results show that the deep (upper) branch of the Brewer-Dobson circulation is affected by the longitudinal distribution of meridional wind, which can affect the distribution of total ozone. Therefore, Fig. 7 shows longitudinal distribution of ozone, and also temperature, at 10 hPa in the middle latitudes (20°-60°N). This distribution is consistent with the two-core structure of meridional wind – in the eastern hemisphere, where the intensified poleward meridional wind transports warmer air and more ozone towards higher latitudes (60°N), the temperature and to a less extent ozone concentration are increasing; in the western hemisphere core the opposite meridional transport reduces temperature and ozone at higher middle latitudes. Thus all studied parameters, meridional wind, geopotential height, zonal wind, temperature and ozone, agree in the main features of the longitudinal variation and provide an internally consistent pattern of the longitudinal variation in the winter middle stratosphere (at 10 hPa) characterized by the two cores of strong meridional wind. This result illustrates limitations of the applicability of the zonal mean approach. To find the main driver of these changes, in future we have to analyze the processes in the lower and higher levels of the atmosphere. To our best knowledge the longitudinal structure of middle stratosphere circulation at middle latitudes has not yet been studied except for Bari et al. (2013), who simulated with the HAMMONIA model for 2001-2006, January a longitudinal structure of residual winds, which resembles our results. They found impact of that longitudinal structure on the Brewer-Dobson circulation and distribution of stratospheric ozone and water vapor. Investigation of the longitudinal dependence of stratospheric zonal winds during SSW events with model HAMMONIA (Miller et al., 2013) demonstrates the asymmetry of the climatological winter and of single events.

We identify statistically significant trends (mostly on the 99 % level) in both core sectors at 10 hPa (Table 1). These trends are positive (strengthening of meridional wind) in 1970-1995 (decreasing ozone content) and negative (weakening of meridional wind) in 1996-2012 (increasing ozone content) for both cores. The strengthening of meridional wind in 1970-1995 (Table 1) and opposite trends/tendencies in 1996-2012 is consistent with some strengthening/weakening of the blocking Aleutian pressure high. This is confirmed by trends in the central part of the blocking Aleutian pressure high; +34.6 m/year for 1970-1995 and -38.3 m/year for 1996-2012, both being significant at the 95% level. The trends are mostly insignificant in the other two sectors (sector not affected by the two-core structure). The analysis was done separately for periods before and after the mid-1990s, when the ozone trend at northern middle latitudes reversed. This analysis confirms similar reversal of trends in the stratospheric wind. However, ozone serves here as an indicator rather than cause of the trend change. Statistical and modeling studies carried out in the European FP5 project CANDIDOZ show that the main cause of this change in ozone trends results from changed dynamical behavior (Harris et al., 2008). This conclusion is supported by behavior of the ozone laminae (Lastovicka et al., 2014).

The above results are the reason why, in section 3.3, we investigate the potential effect of some dynamical factors (SSW and QBO), which could be behind the change of trends of both ozone and wind. The change of the meridional wind trend (from positive to negative in the mid-1990s) occurs independently on SSW or QBO (Table 2). We can connect this with changes of ozone trends. The trends in core structure areas are significant (mainly 99% level) for all four SSW/QBO combinations (Table 2) as well as for all years trend (Table 1). In areas not containing the core structure, more significant trends (95% level) occur for years with than without major SSWs. This result could indicate that the abnormal conditions in the stratosphere during SSW can affect meridional wind trends (B-D circulation and ozone

transport) in areas where meridional wind is weak. Both split and displacement SSWs support stronger meridional wind at high latitudes, which is consistent with our findings.

According to Shindell et al. (1999) the changes of the upper stratospheric wind are caused partly by changes in the solar irradiance. The impact of the 11-yr solar cycle, sometimes in the combination with the QBO, on the stratosphere has been described in many papers (i.e. Salby and Callahan, 2000, Labitzke and Kunze, 2009, Limpasuvan et al. 2004, Naito and Hirota, 1997, Labitzke and van Loon, 1988). The influence of solar activity on the total horizontal wind as well as the meridional component is shown in Table 3. Our results agree with the results of other authors but we specify dependence of solar effect on longitude. The most statistically significant differences in the total horizontal wind can be found again in the two core sectors. The differences are larger in higher latitudes. This result agrees with previous studies that higher latitudes are more affected by changes in solar activity. The analysis of the meridional component does not show any specific features so we can conclude that solar activity affects mainly the total horizontal wind and its zonal component.

5. Conclusions

Based on data from reanalyzes NCEP/NCAR, ERA-Interim and MERRA, the longitudinal distribution of meridional component of stratospheric wind in winter (January) has been examined for 20-60^{o}N. It reveals well pronounced longitudinal distribution of meridional wind at latitudes above 45^{o}N with two cores of strong but opposite meridional winds, one at each hemisphere (eastern and western) at 10 hPa, and a much less pronounced five-core structure at 100 hPa. All three reanalyzes provide the same pattern. In summer, such a well-pronounced core structure is absent. The two-core structure at 10 hPa is not caused by tides, as no differences exist between 00, 06 and 12 UTC results. We have identified the

strong and well-developed large Aleutian pressure high at 10 hPa, which is capable of explaining qualitatively the two-core structure in the longitudinal distribution of meridional wind. The longitudinal distribution of zonal wind, temperature and ozone content is consistent with that of meridional wind and geopotential height, i.e. the middle stratosphere as a whole displays a significant longitudinal distribution at higher middle latitudes. Our results illustrate limitations of the approach via zonal mean values when studying the northern midlatitude middle stratosphere.

The trends of meridional wind are found to be significant in the two core sectors independently on SSW or QBO and mainly insignificant in sectors not containing the two cores. In the period of ozone depletion deepening (1970-1995), the meridional wind in cores intensifies, whereas in the period of recovering ozone concentration (1996-2012) it is also recovering. The influence of the solar cycle can be seen mainly for the west phase of QBO.

Acknowledgements

Authors acknowledge support by the Grant Agency of the Czech Republic, grant P209/10/1792, by the Ministry of Education, Youth and Sports of the Czech Republic, grant LD 12070, and by the COST ES1005 project (TOSCA).

References

Baldwin, M.P., and Dunkerton, T.J.: Propagation of the arctic oscillation from the stratosphere to the troposphere, J. Geophys. Res., 104, 30937-30946, 1999.

Baldwin, M., Shuckburgh, D. Norton, E., Thompson, and W., Gillett, G.: Weather from the Stratosphere? Science, 301, 317-318, 2003.

Baron, P., Murtagh, D. P., Urban, J., Sagawa, H., Ochiai, S., Kasai, Y., Kikuchi, K., Khosrawi, F., Kornich, H., Mizobuchi, S., Sagi, K and Yasui, M.: Observation of

398 horizontal winds in the middle-atmosphere between 30◦ S and 55◦ N during the northern
399 winter 2009–2010, Atmos. Chem. Phys., 13, 6049-6064, doi:10.5194/acp-13-6049-2013,
400 2013.
401 Butchart, N.: The Brewer-Dobson circulation, Rev. Geophys., 52, 157-184, doi:
402 10.1002/2013RG00448, 2014.
403 Deckert, R., and Dameris, M.: Higher tropical SSTs strengthen the tropical upwelling via
404 deep convection, Geophys. Res. Lett, *35*, L10813, doi: 10.1029/2008L033719, 2008.
405 Dee, D. P., Uppala, S. M., Simmons, A. J., Berrisford, P., Poli, P., Kobayashi, S., Andrae, U.,
406 Balmaseda, M. A., Balsamo, G., Bauer, P., Bechtold, P., Beljaars, A. C. M., van de Berg,
407 L., Bidlot, J., Bormann, N., Delsol, C., Dragani, R., Fuentes, M., Geer, A. J., Haimberger,
408 L., Healy, S. B., Hersbach, H., Hólm, E. V., Isaksen, L., Kållberg, P., Köhler, M.,
409 Matricardi, M., McNally, A. P., Monge-Sanz, B. M., Morcrette, J.-J., Park, B.-K., Peubey,
410 C., de Rosnay, P., Tavolato, C., Thépaut, J.-N., and Vitart, F.: The ERA-Interim reanalysis:
411 configuration and performance of the data assimilation system, Q. J. Roy. Meteorol. Soc.,
412 137, 553–597, 2011.
413 Demirhan Bari, D., Gabriel, A., Körnich, H., Peters, D. W. H.: The effect of zonal
414 asymmetries in the Brewer-Dobson circulation on ozone and water vapor distributions in
415 the northern middle atmosphere, J. Geophys. Res. Atmos., 118, 3447-3466, doi:
416 10.1029/2012JD017709, 2013
417 Engel, A., Möbius, T., Bönisch, H., Schmidt, U., Heinz, R., Levin, I., Atlas, E., Aoki, S.,
418 Nakazawa, T., Sugawara, S., Moore, F., Hurst D., Elkins J., Schauffler S., Andrews A.,
419 and Boering K.: Age of stratospheric air unchanged within uncertainties over the past 30
420 yr. Nat. Geosci., 2, 28–31, doi:10.1038/ngeo388, 2009.
421 Gray, L.J., Beer, J., Geller, M., Haigh, J.D., Lockwood, M., Matthes, K., Cubasch, U.,
422 Fleitmann, D., Harrison, G., Hood, L., Luterbacher, J., Meehl, G.A., Shindell, D., van

Geel, B., and White, W.: Solar influences on climate, Rev. Geophys., 48, RG4001, doi: 10.1029/2009RG000282, 2010.

Hamilton, K., Vial, F., and Stenchikov, G.: Longitudinal variation of the stratospheric quasi-biennial oscillation, J. Atmos. Sci., 61 (4), 383-402, 2004.

Harris, N. R. P., Kyrö, E. Staehelin, J., et al.: Ozone trends at northern mid- and high latitudes — A European perspective, Ann. Geophys., 26, 1207–1220, doi: 10.5194/angeo-26-1207-2008, 2008.

Hartmann, D. L., Wallace, J. M., Limpasuvan, V., Thompson, D. W., and Holton, J. R.: Can ozone depletion and global warming interact to produce rapid climate change? Proc. Nat. Acad. Sci., 97(4), 1412-1417, 2000.

Hildebrand, J., Baumgarten, G., Fiedler, J., Hoppe, U.-P., Kaifler, B., Lubken, F.-J., and Williams, B. P.: Combined wind measurements by two different lidar instruments in the Arctic middle atmosphere, Atmos. Meas. Tech., 5, 2433–2445, 2012.

Holton, J. R., and Alexander, M. J. The role of waves in transport circulation of the middle atmosphere. Geophys. Monogr. Ser., vol. 123, AGU, Washington DC, 21-35, 2000.

Kistler, R., Collins W. Kalnay, E., et al. The NCEP 50-year reanalysis: Monthly means CDrom and documentation. Bull. Am. Meteorol. Soc. 82 (2), 247-267, 2001.

Kodera, K., Yamazaki, K., Chiba, M., & Shibata, K.: Downward propagation of upper stratospheric mean zonal wind perturbation to the troposphere. Geophys. Res. Lett., 17(9), 1263-1266, doi: 10.1029/L017i009p01263, 1990.

Kozubek, M., Laštovička, J., and Križan, P.: Differences in mid-latitude stratospheric winds between reanalysis data and versus radiosonde observations at Prague, Ann. Geophys., 32, 353-366, doi: 10.5194/angeo-32-353-2014, 2014.

446 Labitzke, K., and van Loon, H.: Associations between the 11-year solar cycle, the QBO and
447 the atmosphere: Part I. The troposphere and stratosphere in the Northern Hemisphere
448 winter, J. Atmos. Terr. Phys., 50, 197–206, 1988
449 Labitzke, K., and Kunze, M.: Variability in the stratosphere: The Sun and the QBO,
450 in Climate and Weather of the Sun-Earth System (CAWSES): Selected Papers from the
451 Kyoto Symposium, edited by K. S. T. Tsuda, R. Fujii, and M. Geller, pp. 257–278,
452 TERRAPUB, Tokyo, 2009.
453 Lastovicka, J., Solomon, S.C., and Qian, L.: Trends in the Neutral and Ionized Upper
454 Atmosphere, Space Sci. Rev., 168, 113–145, doi: 10.1007/s11214-011-9799-3, 2012.
455 Lastovicka, J., Krizan, P., and Kozubek, M.: Long-term trends in the northern extratropical
456 ozone laminae with focus on European stations, J. Atmos. Sol.-Terr. Phys., 120, 88-95,
457 http://dx.doi.org/10.1016/j.jastp.2014.09.006, 2014.
458 Limpasuvan, V., Thompson, D. W., and Hartmann, D. L. The life cycle of the Northern
459 Hemisphere sudden stratospheric warmings. J. Clim., 17(13), 2584-2596, 2004.
460 Lin, P., and Fu, Q.: Changes in various branches of the Brewer–Dobson circulation from an
461 ensemble of chemistry climate models. J. Geophys. Res. Atmos, 118(1), 73-84, doi:
462 10.1029/2012JD018813, 2013.
463 Marshall, A. G., and Scaife, A. A. Impact of the QBO on surface winter climate. J. Geophys.
464 Res. Atmos., 114, D18, doi: 10.1029/2009JD011737, 2009
465 Matsuno, T.: Vertical propagation of stationary planetary waves in the winter Northern
466 Hemisphere. J. Atmos. Sci., 27(6), 871-883, 1970.
467 Miller, A., Schmidt, H., and Bunzel, F.: Vertical coupling of the middle atmosphere during
468 stratospheric warming events. J. Atmos. Sol.-Terr. Phys., 97, 11-21,
469 http://dx.doi.org/10.1016/j.jastp.2013.02.008, 2013.

Mlch, P.: Total ozone response to major geomagnetic storms during non-winter periods. Studia geoph. Geod., 38 (4), 423-429, 1994.

Monier, E. and Weare, B. C.: Climatology and trends in the forcing of the stratospheric ozone transport. Atmos. Chem. Phys., 11, 6311-6323, doi: 10.5194/acp-11-6311-2011, 2011a.

Monier, E. and Weare, B. C.: Climatology and trends in the forcing of the stratospheric zonal-mean flow. Atmos. Chem. Phys., 11, 12751-12771, doi:10.5194/acp-11-12751-2011, 2011b.

Naito, Y., and Hirota, I. Interannual variability of the northern winter stratospheric circulation related to the QBO and the solar cycle. Journal of the Meteorological Society of Japan, 75(4), 925-937, 1997

Oberländer, S., Langematz, U., and Meul, S.: Unravelling impact factors for future changes in the Brewer- Dobson circulation. J. Geophys. Res. Atmos, *118*, 10,296-10,312, doi: 10.1002/jgrd.50775, 2013.

Oman, L., Waugh, D. W., Pawson, S., Stolarski, R. S., & Newman, P. A.: On the influence of anthropogenic forcings on changes in the stratospheric mean age. J. Geophys. Res. Atmos *(1984–2012)*, *114*, D03105, doi: 10.1029/2008JD010378, 2009.

Ortland, D. A., Skinner, W. R., Hays, P. B., Burrage, M. D., Lieberman, R. S., Marshall, A. R., and Gell, D. A.: Measurements of stratospheric winds by the High Resolution Doppler Imager. J. Geophys. Res., 101, 10351–10363, 1996.

Pommereau, J.-P., Goutail, F., Lefèvre, F., Pazmino, A., Adams, C., Dorokhov, V., Eriksen, P., Kivi, R., Stebel, K., Zhao, X., and van Roozendael, M.: Why unprecedented ozone loss in the Arctic in 2011? Is it related to climate change?, Atmos. Chem. Phys., 13, 5299-5308, doi: 10.5194/acp-13-5299-2013, 2013.

493 Rüfenacht, R., Kampfer, N., and Murk, A.: First middle atmospheric zonal wind profile
494 measurements with a new ground-based microwave Doppler-spectro-radiometer, Atmos.
495 Meas. Tech., 5, 2647–2659, 2012
496 Salby, M., Callahan, P.: Connection between the Solar Cycle and the QBO: The missing link,
497 J. Clim., 13(14), 2652-2662, 2000.
498 Scaife, A. A., Spangehl, T., Fereday, D. R., Cubasch, U., Langematz, U., Akiyoshi, H.,
499 Slimane, B., Breasicke, P., Butchard, N., Chipperfield, M. P., Gettelman, A., Hardiman, S.
500 C., Michou, M., Rozanov, E. and Shepherd, T. G.: Climate change projections and
501 stratosphere–troposphere interaction. *Clim. Dynamics*, *38*(9-10), 2089-2097, 2012.
502 Shepherd, T.G. Transport in the middle atmosphere. J. Meteorol. Soc. Jpn. II, 85B,
503 165-191, 2007.
504 Shepherd, T.G. Dynamics, stratospheric ozone, and climate change. Atmos. Ocean, 46,
505 117-138, 2008.
506 Shindell, D., Rind, D., Balachandran, N., Lean, J., & Lonergan, P.: Solar cycle variability,
507 ozone, and climate. Science, 284(5412), 305-308, 1999.
508 Sigmond, M., Scinocca, J. F, and Kushner, P. J. Impact of the stratosphere on the tropospheric
509 climate change. Science, 301, 317-318, 2008.
510 Stiller, G. P., von Clarmann, T., Haene,l F., Funke, B., Glatthor, N., Grabowski, U.,
511 Kellmann, S., Kiefer, M., Linden, A., Lossow, S., and Lopez-Puertas, M.: Observed
512 temporal evolution of global mean age of stratospheric air for the 2002 to 2010 period.
513 Atmos. Chem. Phys., 12, 3311–3331, doi:10.5194/acp-12-331-2012, 2012.
514 Wang, L., and Chen, W. Downward arctic oscillation signal associated with moderate weak
515 stratospheric polar vortex and the cold December 2009. Geophys. Res. Lett., 37, L09707,
516 doi: 10.1029/2010GL042659, 2010.

Weare, B. C.: Tropospheric-stratospheric wave propagation during El Niño-Southern Oscillation. J. Geophys. Res., 115, D18122, doi: 10.1029/2009JD013647, 2010.

Table 1: Winter (December-February) trends (m/s per year) of meridional wind speed for two periods (1970-1995 and 1996-2012). Pressure level 10 hPa. 70-95 means 1970-1995 and 95-12 means 1995-2012 Trends significant on the 99% level are highlighted by bold numbers and red; trends significant on the 95% level are in italics and green. Sectors 100°-160°E and 140°-80°W are the sectors with cores in meridional wind.

10 hPa												
latitude	50°N					55N			60°N			
sector	**100° E-160° E**	**160° E-140° W**	**140° W-80° W**	**80°W - 100° E**	**100°E-160°E**	**160° E-140° W**	**140° W-80° W**	**80° W-100° E**	**100° E-160° E**	**160° E-140° W**	**140° W-80° W**	**80° W-100° E**
70-95	*0.42*	0.10	*0.39*	0.07	**0.48**	0.11	*0.42*	0.03	*0.47*	0.09	*0.42*	0.04
95-12	**-0.71**	-0.15	**-0.68**	-0.09	**-0.68**	-0.19	**-0.74**	-0.06	**-0.79**	-0.12	**-0.67**	-0.10

Table 2: Winter (December-February) trends (m/s per year) of the meridional wind speed for two periods (1970-1995 and 1996-2012). Major SSW- only years when the major SSWs (according to WMO definition) occur; no SSW – years when no SSW occurs; east QBO - only years under the east phase of QBO ; west QBO - only years under the west phase of QBO. Pressure level 10 hPa. 70-95 means 1970-1995 and 95-12 means 1995-2012. Trends

significant on the 99% level are highlighted by bold numbers and red; trends significant on the 95% level are in italics and green.

10 hPa													
latitude	50°N					55N			60°N				
sector	**100° E-160° E**	**160° E-140° W**	**140° W-80° W**	**80°W - 100° E**	**100°E-160°E**	**160° E-140° W**	**140° W-80° W**	**80° W-100° E**	**100° E-160° E**	**160° E-140° W**	**140° W-80° W**	**80° W-100 °E**	
70-95	**0.52**	*0.21*	*0.49*	0.15	**0.57**	0.15	**0.54**	0.12	**0.60**	0.11	**0.55**	0.10	**major SSW**
95-12	**-0.61**	-0.19	**-0.63**	-0.10	**-0.61**	*-0.27*	**-0.67**	*-0.24*	**-0.64**	-0.22	**-0.59**	*-0.26*	
70-95	**0.39**	*0.23*	**0.46**	*0.20*	**0.43**	0.19	**0.51**	0.15	**0.49**	0.16	**0.56**	*0.18*	**no SSW**
95-12	**-0.71**	-0.08	**-0.42**	-0.05	**-0.6**	-0.11	**-0.49**	-0.08	**-0.64**	-0.13	**-0.56**	-0.1	
70-95	0.37	0.14	0.35	0.09	*0.39*	*0.17*	**0.42**	*0.19*	**0.43**	0.19	**0.48**	0.23	**east QBO**
95-12	**-0.44**	*-0.24*	**-0.40**	*-0.19*	**-0.48**	-0.16	**-0.46**	-0.11	**-0.53**	-0.12	**-0.51**	-0.09	
70-95	**0.34**	*0.19*	**0.49**	*0.20*	**0.41**	*0.24*	**0.55**	0.21	***0.39***	*0.25*	**0.59**	*0.27*	**west QBO**
95-12	**-0.50**	-0.08	**-0.64**	-0.04	**-0.54**	-0.12	**-0.62**	-0.09	**-0.57**	-0.17	**-0.68**	-0.12	

Table 3: Winter (December-February) differences of wind speed (m/s) for different latitudes and sectors during the whole period. Top panel shows the total horizontal wind speed for 10 hPa, bottom panel the v (meridional) wind component for 10 hPa. Min-east: years under solar minimum and the east phase of QBO conditions; min-west: years under solar minimum and

543 the west phase of QBO; the same for solar maximum conditions. Significant differences on

544 the 95% level are highlighted by bold numbers.

	50°N				55°N				60°N				latitude
	100° E-160° E	**160° E-140° W**	**140° W-80°W**	**80°W - 100° E**	**100° E-160° E**	**160° E-140° W**	**140° W-80° W**	**80°W - 100° E**	**100° E-160° E**	**160° E-140° W**	**140° W-80° W**	**80°W - 100° E**	**sector**
(min/east)-(min/west)	**-1.07**	-0.08	**-1.47**	-0.03	**-1.89**	-0.28	**-1.73**	-0.23	**-2.77**	-0.57	**-2.05**	-0.53	**10 hPa**
(max/east)-(max/west)	0.33	-0.27	1.26	-0.46	0.66	-0.42	1.17	-0.44	1.04	-0.18	0.76	-0.27	
(min/west)-(max/west)	**2.02**	0.38	**1.39**	0.51	**2.76**	**0.81**	**1.84**	0.72	**3.19**	**1.08**	**2.23**	1.01	
(min/east)-(max/east)	0.62	**0.96**	**-1.36**	**1.02**	-0.39	0.75	-1.19	0.81	-0.71	0.64	-0.92	0.56	
(min/east)-(min/west)	-0.01	0.34	**-0.63**	0.60	-0.11	-0.29	-0.73	**0.79**	-0.26	**1.14**	**-0.84**	**1.12**	**10 hPa v**
(max/east)-(max/west)	-0.38	0.2	0.15	0.09	-0.40	-0.52	0.14	0.10	-0.43	0.18	0.17	0.14	
(min/west)-(max/west)	-0.17	0.42	**1.17**	-0.73	-0.20	-0.17	**1.39**	**-0.86**	-0.18	-0.95	**1.57**	**-0.99**	
(min/east)-(max/east)	0.19	-0.29	0.39	-0.22	0.09	-0.11	0.49	-0.17	-0.01	-0.17	0.57	-0.11	

545

546

547

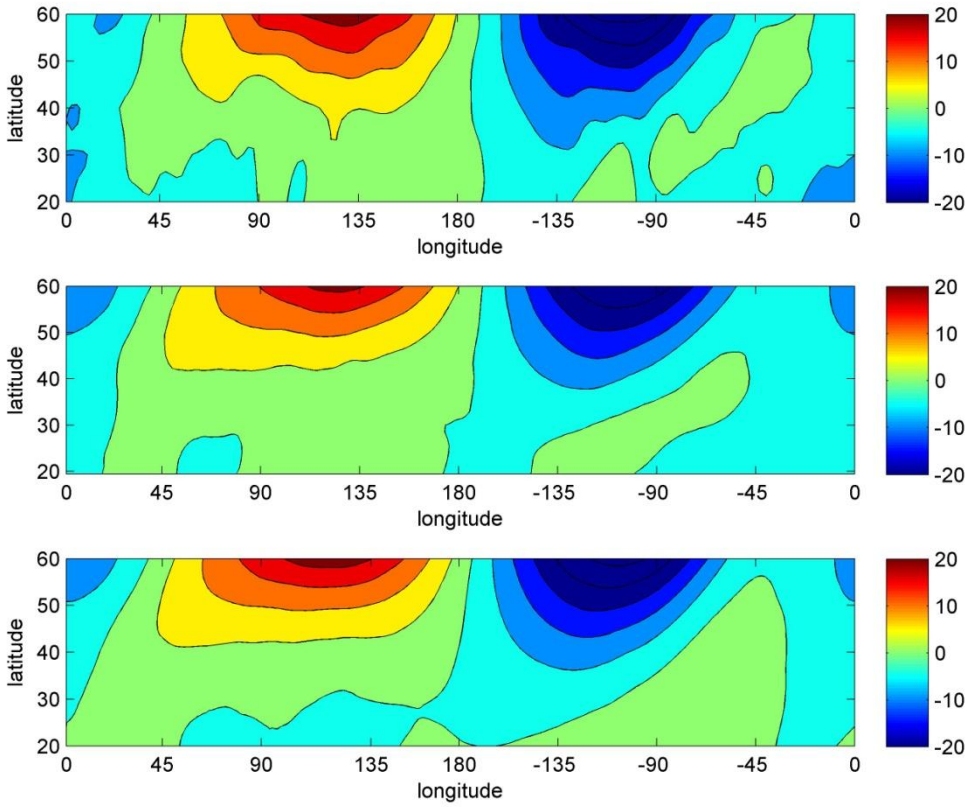

548

549 **Figure 1** Plot of average meridional wind speed (m/s) component for January, 20-60°N,
550 180°E-180°W, 10 hPa. Top panel NCEP/NCAR (1958-2012), middle ERA Interim (1979-
551 2012), and bottom MERRA (1979-2012). Positive values (poleward wind - red), negative
552 values (equatorward wind – blue).

553

554

555

556

557

558

559

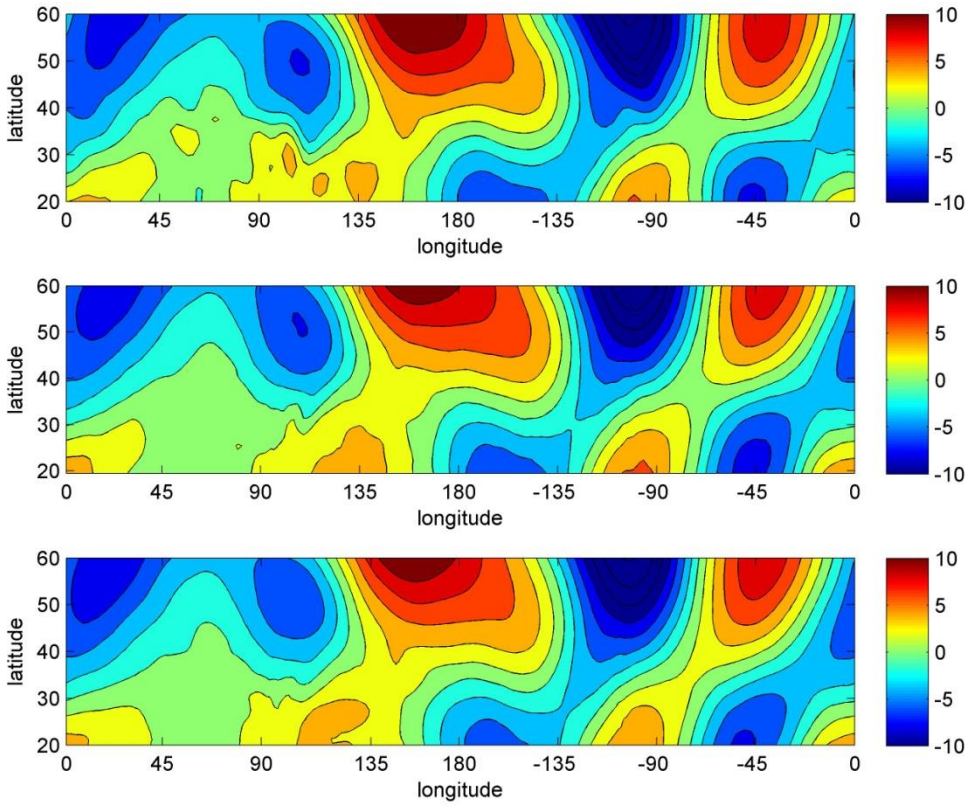

560

561 **Figure 2** The same as Fig.1 but for 100 hPa.

562

563

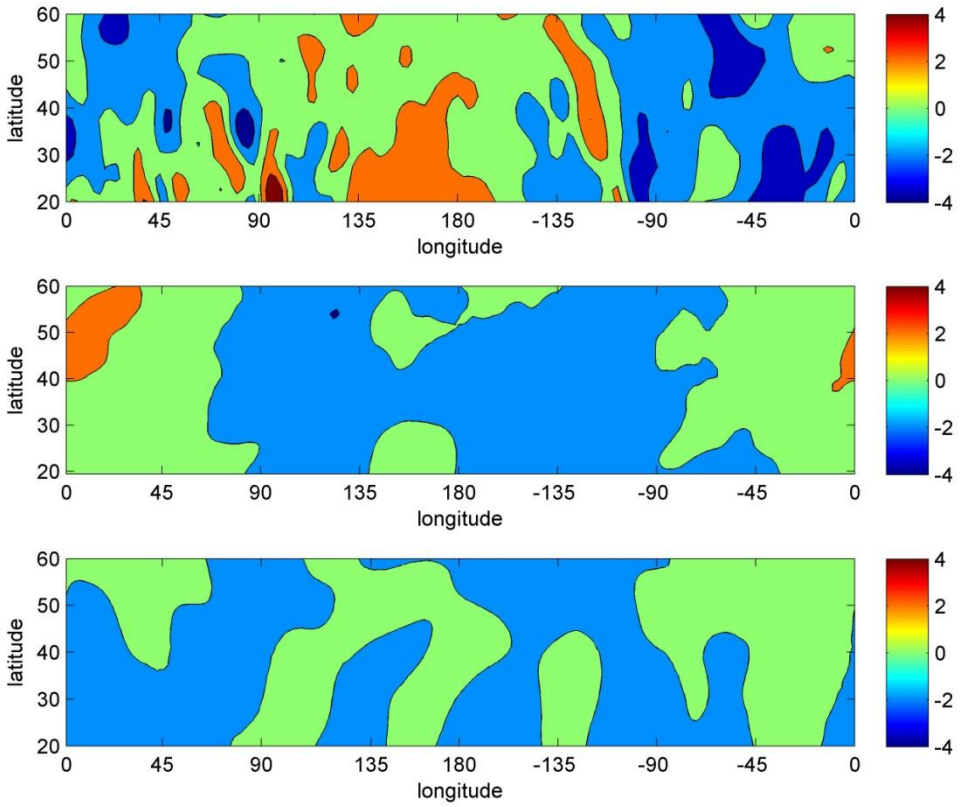

564

565 **Figure 3:** The same as Fig. 1 but for July. Positive values (poleward wind -red), negative

566 values (equatorward wind - blue).

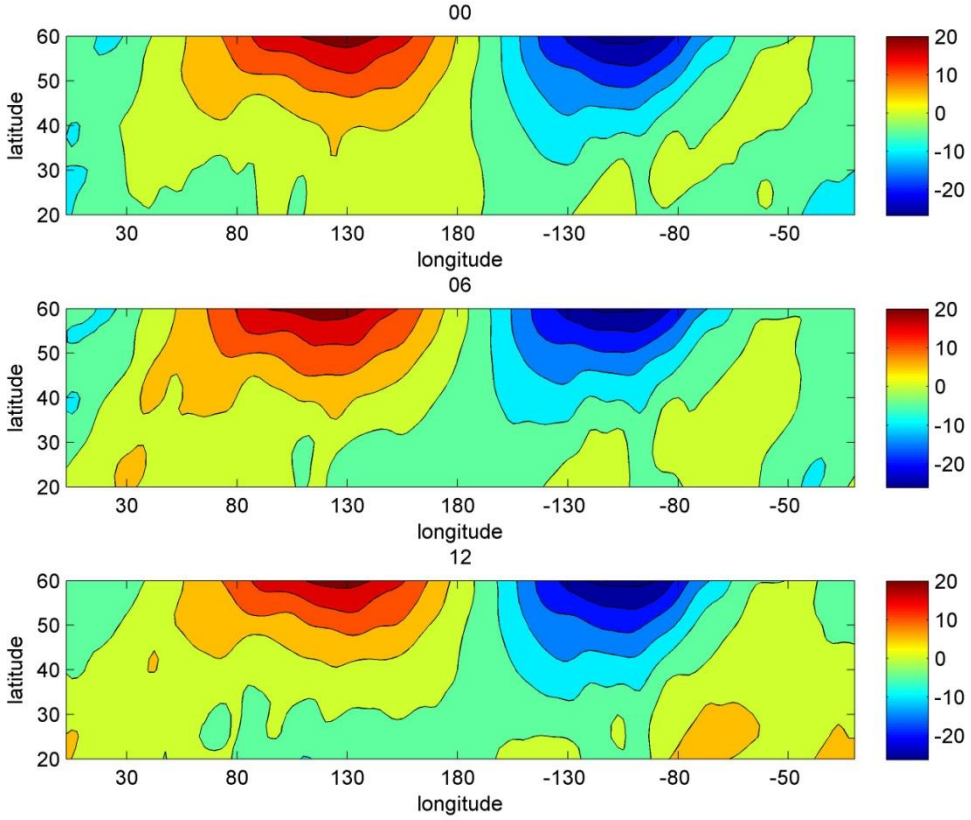

567

568 **Figure 4:** Plot of average meridional wind speed (m/s) component at 10 hPa for January,
569 1958-2012, 20-60°N, 180°E-180°W. Top panel 00 UTC, middle 06 UTC, and bottom 12
570 UTC. Positive values (poleward wind - red), negative values (equatorward wind - blue),
571 NCEP/NCAR reanalysis only.

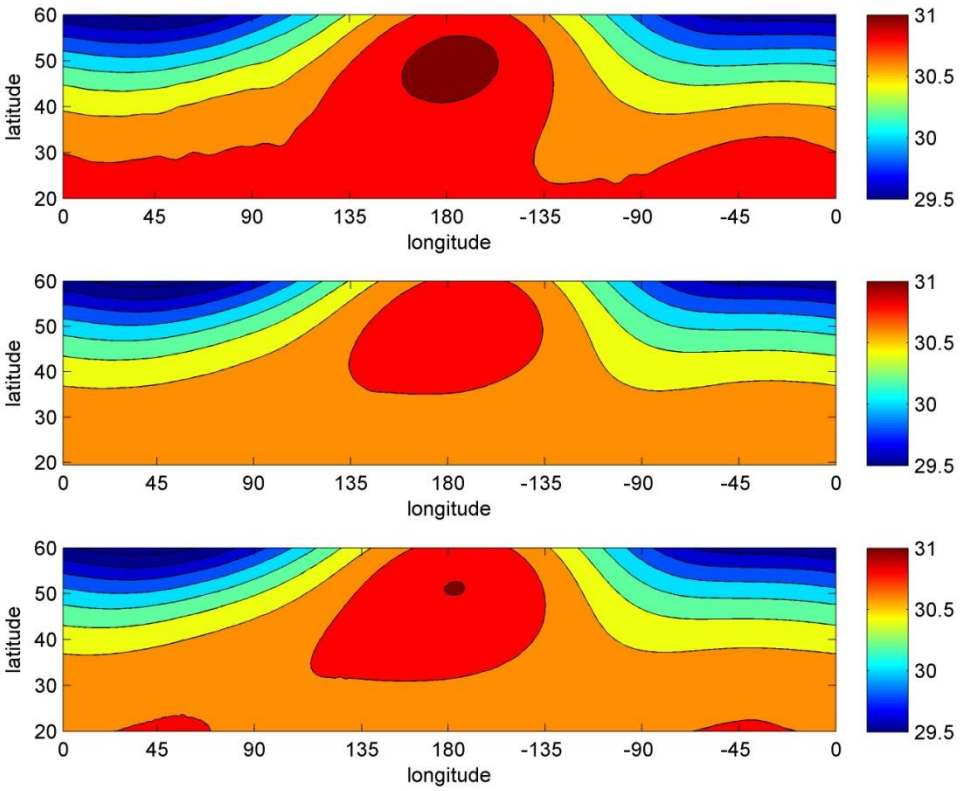

572

573 **Figure 5:** Plot of average geopotential height (km) for January, 1958-2012, 20-60°N, 180°E-

574 180°W. Top panel NCEP/NCAR (1958-2012), middle ERA Interim (1979-2012), and bottom

575 MERRA (1979-2012).

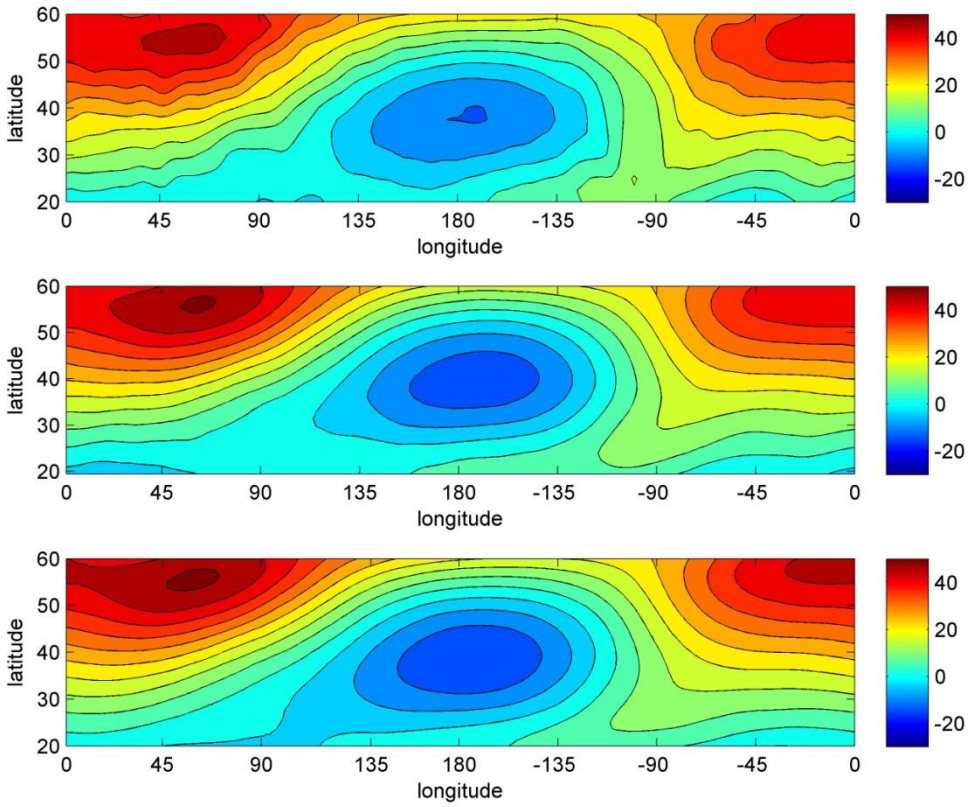

576

577 **Figure 6** Plot of average zonal wind speed (m/s) component for January, 20-60°N, 180°E-
578 180°W, 10 hPa. Top panel NCEP/NCAR (1958-2012), middle ERA Interim (1979-2012), and
579 bottom MERRA (1979-2012). Positive values (eastward wind - red), negative values
580 (westward wind - blue).

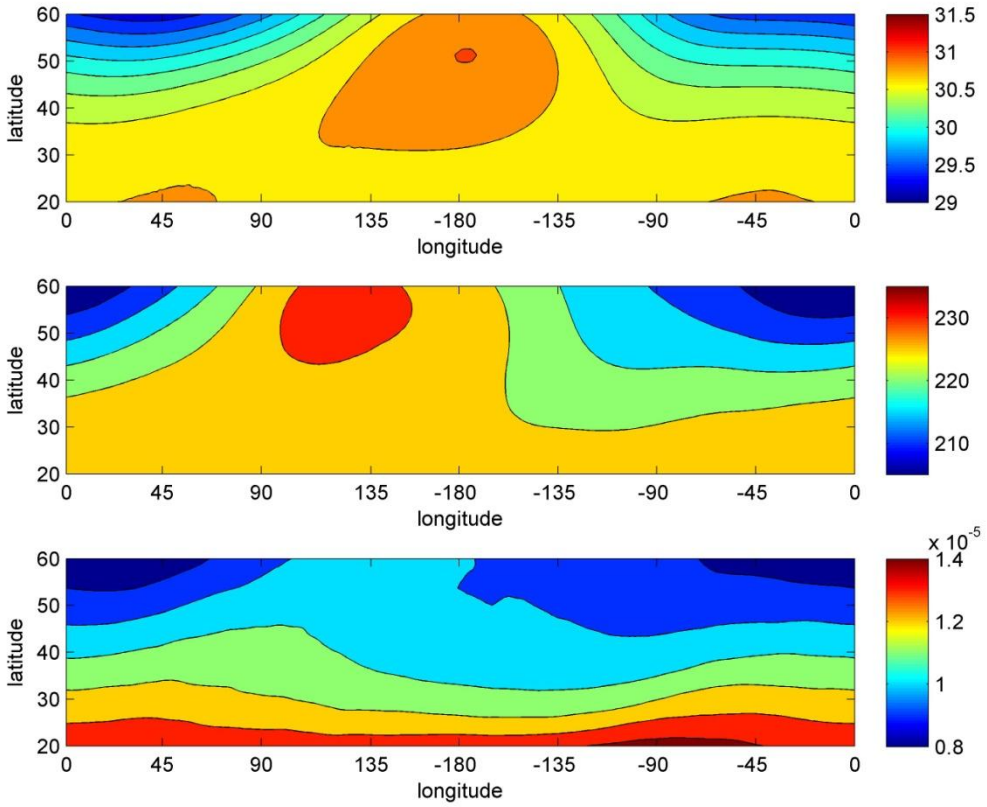

581

582 **Figure 7** Plot of average geopotential height (km, top panel), temperature (K, middle panel)

583 and ozone mixing ratio (ppmv, bottom panel) for January, 20-60°N, 180°E-180°W, 10 hPa.

584

585